PERGAMON

Carbon 41 (2003) 2459–2469

CARBON

Carbon black dispersions as thermal pastes that surpass solder in providing high thermal contact conductance

Chia-Ken Leong, D.D.L. Chung*

Composite Materials Research Laboratory, University at Buffalo, State University of New York, Buffalo, NY 14260-4400, USA

Received 7 May 2003; accepted 31 May 2003

Abstract

Carbon black dispersions based on polyethylene glycol (PEG) or di(ethylene glycol) butyl ether, along with dissolved ethyl cellulose, provide thermal pastes that are superior to solder as thermal interface materials. The thermal contact conductance of the interface between copper disks reaches 3×10^5 W/m^2 °C, compared to 2×10^5 W/m^2 °C for a tin–lead–antimony solder. The pastes based on PEG are superior to those based on butyl ether in their thermal stability above 100 °C. Carbon black is superior to materials that are more conductive thermally (graphite, diamond and nickel particles, and carbon filaments) in providing thermal pastes of high performance. The performance of thermal pastes and solder as thermal interface materials is mainly governed by their conformability and spreadability rather than their thermal conductivity.

Keywords: A. Carbon black; C. Thermal analysis; D. Thermal conductivity

1. Introduction

With the miniaturization and increasing power of microelectronics, heat dissipation has become critical to the performance, reliability and further miniaturization of microelectronics. Heat dissipation from microelectronics is most commonly performed by thermal conduction. For this purpose, a heat sink, which is a material of high thermal conductivity, is commonly used. In order for the heat sink to be well utilized, the thermal contact between the heat sink and the heat source (e.g., a substrate with a semiconductor chip on it) should be good [1,2]. A thermal fluid or paste is commonly applied at the interface to enhance the thermal contact [3]. The fluid or paste is a material that has high conformability so that it can conform to the surface topography of the mating surfaces, thereby avoiding air gaps (which are thermally insulating) at the interface. The fluid or paste must be highly spreadable, so that the thickness of the paste after application is very thin (just enough to fill the valleys in the surface topography of the mating surfaces). Preferably the fluid or paste is thermally conductive as well. Although much attention has been given to the development of heat sink materials, relatively little attention has been given to the development of thermal fluids or pastes.

The most common thermal fluid is mineral oil. As a fluid, it is highly conformable and spreadable, but it has a low thermal conductivity. The most common thermal paste is silicone filled with thermally conductive particles [4–7]. Due to the filler, it is relatively high in thermal conductivity, but it suffers from poor conformability and poor spreadability. Thermal fluids and pastes used in previous studies are not as effective as solder (applied when it is molten) [8,9], but they do not require heating, which is required for the use of solder.

This paper is focused on the addition of a thermally conductive filler to organic vehicles for the purpose of providing a thermal paste which is conformable, spreadable and relatively high in thermal conductivity. The fillers included in this study are carbons (carbon black, 1 and 5 μm graphite particles, 0.1 μm diameter discontinuous carbon filaments and 25 μm diamond particles) and 1 and 3 μm nickel particles. Of all these fillers, carbon black [10], which is porous, is the only type that is itself spreadable (compressible). The spreadability [11–13], probably along with wettability, is believed to be the

---

*Corresponding author. Tel.: +1-716-654-2593x2243; fax: +1-716-645-3875.

E-mail address: ddlchung@eng.buffalo.edu (D.D.L. Chung).

0008-6223/03/$ – see front matter © 2003 Elsevier Ltd. All rights reserved.
doi:10.1016/S0008-6223(03)00247-1

reason behind the superior performance of carbon black compared to all the other fillers investigated. Furthermore, the porosity of a carbon black particle allows penetration of the vehicle into a carbon black particle. The porosity, probably along with wettability, enables the resulting paste to have high fluidity, as previously shown for the case of oil as the vehicle [14–18].

Organic vehicles are commonly used as the suspending medium for dispersed inorganic particles in pastes [19–22]. An organic vehicle system may consist of a solvent (such as butyl ether [23]) and a solute (such as ethyl cellulose [22]), which serves to enhance the dispersion and suspension [19]. Ethyl cellulose offers the further advantage of its slight conductivity [24,25].

Another organic vehicle is polyethylene glycol (PEG, a polymer) of low molecular weight (400 amu) [8], which is different from silicone in that its viscosity is lower. By using PEG in conjunction with boron nitride particles as a thermal paste between copper disks, a thermal contact conductance of 1.9×10^5 W/m^2 °C has been produced [8]. This value is higher than that obtained by using a thermal paste involving silicone and boron nitride powder (1.1×10^5 W/m^2 °C) [8], but is lower than that obtained by using a tin–lead–antimony solder (applied in the molten state) (2.1×10^5 W/m^2 °C) [8].

All thermal pastes previously reported are inferior to solder in providing high thermal contact conductance. By using carbon black as the thermally conductive ingredient, we have attained thermal pastes that are superior to solder in providing high thermal contact conductance.

This work provides a comparative study of various organic vehicles, namely PEG with 0–15 vol.% dissolved ethyl cellulose and di(ethylene glycol) butyl ether with 0–40 vol.% dissolved ethyl cellulose. The comparative evaluation pertains both to the effectiveness of the thermal paste and the temperature resistance, as both attributes are relevant to the applications of thermal pastes.

Carbon black is used as a low-cost electrically conductive filler in polymers [26,27]. Most commonly, it is used as a reinforcement in rubber [28–33]. In addition, it is used in electrochemical electrodes [34,35], inks [36–38], lubricants [39–42], fuels [43–45], and pigments [46,47]. This paper provides a new application for carbon black. The thermal paste involving carbon black is not only useful for microelectronic cooling, but also for heat pipes for tapping geothermal energy [48,49] and for thermal fluid heaters for providing indirect process heat [50].

2. Experimental methods

2.1. Materials

The PEG [or $HO(CH_2CH_2O)_nH$] used as an organic vehicle was PEG 400 from EM Science (Gibbstown, NJ, USA). It had an average molecular weight of 400 amu; this average value corresponds to n~8.68. It was a liquid at room temperature and optionally contained ethyl cellulose (E8003; Sigma, St. Louis, MO, USA) at either 3 or 5 vol.%. The ethyl cellulose was a white powder that was dissolved in the vehicle. It served to improve the dispersion and suspension of the solids in the pastes.

The other organic vehicle used was di(ethylene glycol) butyl ether (from Aldrich, Milwaukee, WI, USA). It optionally contained ethyl cellulose at 10, 20, 30 or 40 vol.%, from Sigma.

The carbon black used was Vulcan XC72R GP-3820 from Cabot (Billerica, MA, USA). This carbon black was chosen due to its electrical conductivity and easy dispersion. It was a powder with an average particle size of 30 nm, a nitrogen specific surface area of 254 m^2/g, a maximum ash content of 0.2% and a density of 1.7–1.9 g/cm^3. The carbon black powder was mixed with a vehicle by hand stirring to form a uniform paste. Other thermally conductive solids, all used at 0.27 vol.% for the sake of comparison, were graphite particles [Asbury Graphite Mills, Asbury, NJ, USA (i) artificial graphite, Grade Ultra Fine 440, 99.4% typical carbon content, 1 μm typical size, and (ii) natural crystalline flake, Grade Micro 850, 98.5% minimum carbon content, 5 μm typical size], carbon filaments (Applied Sciences, Cedarville, OH, USA, 0.1 μm diameter, >100 μm length, with intertwined morphology and fishbone texture), 1 μm nickel particles (INCO, Missassauga, Canada, Type 210), 3 μm nickel particles (Novamet Specialty Products, Wyckoff, NJ, USA, Type 525, 15–20 μm length), and 25 μm diamond particles (Warren Superabrasives, Olyphant, PA, USA, Type MB).

The pastes were prepared by first dissolving ethyl cellulose (if applicable) in the vehicle (either PEG or butyl ether). The dissolution was performed at room temperature for butyl ether, but at about 60 °C (with heat provided by a hot plate) for PEG. The heating in the case of PEG was applied to hasten the dissolution of ethyl cellulose. After this, the thermally conductive solid ingredient was added. Mixing was conducted by using a ball mill and stainless steel balls for 30 min. After mixing, the paste was placed in a vacuum chamber (which involved a mechanical vacuum pump) without heating for the purpose of air bubble removal.

2.2. Thermal contact conductance measurement

Various thermal pastes were sandwiched between the flat surfaces of two copper disks (both surfaces of each disk having been mechanically polished by using 0.05 μm alumina particles), which had a diameter of 12.6 mm and a thickness of 1.16 mm for one disk and 1.10 mm for the other disk. The thermal contact conductance between the two copper disks with and without a thermal interface material was measured using the transient laser flash method [8,9,51,52]. The pressure on the sandwich was controlled at 0.46, 0.69 and 0.92 MPa. This is because the pressure affects the thermal contact conductance, even for a material which is not resilient [9]. The thickness of the thermal interface material was 25 μm or less. The uniform distribution of the paste in the plane of the sandwich was made possible by the fluidity of the paste and the use of pressure. The interface material thickness was obtained by subtracting the thicknesses of the two copper disks from the thickness of the sandwich. All thicknesses were measured using a micrometer. The interface material thickness in all cases was the same before and after the conductance measurement.

For the sake of comparison, solder (applied in the molten state) was also used as a thermal interface material. The solder was tin–lead–antimony (63Sn–36.65Pb–0.35Sb), with activated Rosin flux core, and was supplied as Solder Type 361A-20R by the Measurements Group (Raleigh, NC, USA). Molten solder at a temperature of 187 °C, as measured by using a Type-T thermocouple, was sandwiched between copper disks that had been preheated to this temperature also. This temperature was above the liquidus temperature of 183 °C. The heat was provided by a hot plate. The copper–solder–copper sandwich was allowed to cool on the hot plate with the power off under a slight pressure of 63 kPa. The thickness of the solder layer was also 25 μm or less.

The finite element program ABAQUS (Abaqus, OH, USA) was used to calculate the thermal contact conductance through temperature vs. time curves, which were experimentally obtained. The calculation [9] assumed no thickness and no heat capacity for the interface between the two copper disks. In addition, it assumed no heat transfer between specimen and environment except for the absorption of laser energy by the specimen. Moreover, it assumed that the laser energy was uniformly absorbed on the surface of the specimen, that the heat flow was one-dimensional, and that the thermal contact conductance between the two copper disks was uniform. The validity of these assumptions is supported by the calibration results and error analysis given below.

A Coherent General Everpulse Model 11 Nd glass laser with a pulse duration of 0.4 ms, a wavelength of 1.06 μm and a pulse energy up to 15 J was used for impulse heating. The laser power was adjusted to allow the temperature rise of the specimen to be between 0.5 and 1.0 °C. The upper surface of disk 1 on which the laser beam would directly hit had been coated with carbon by using a flame in order to increase the extent of laser energy absorption relative to the extent of reflection (Fig. 1). An E-type thermocouple (1) was attached to the back surface of disk 2 to monitor the temperature rise. Another thermocouple (2) of the same type was placed ~30 cm above the specimen holder to detect the initial time when the laser beam came out. A National Instruments DAQPad-MIO-16XE-50 data acquisition board with a data acquisition rate up to 20,000 data points per second at 16 bites resolution, along with NI-DAQ interface software coded in

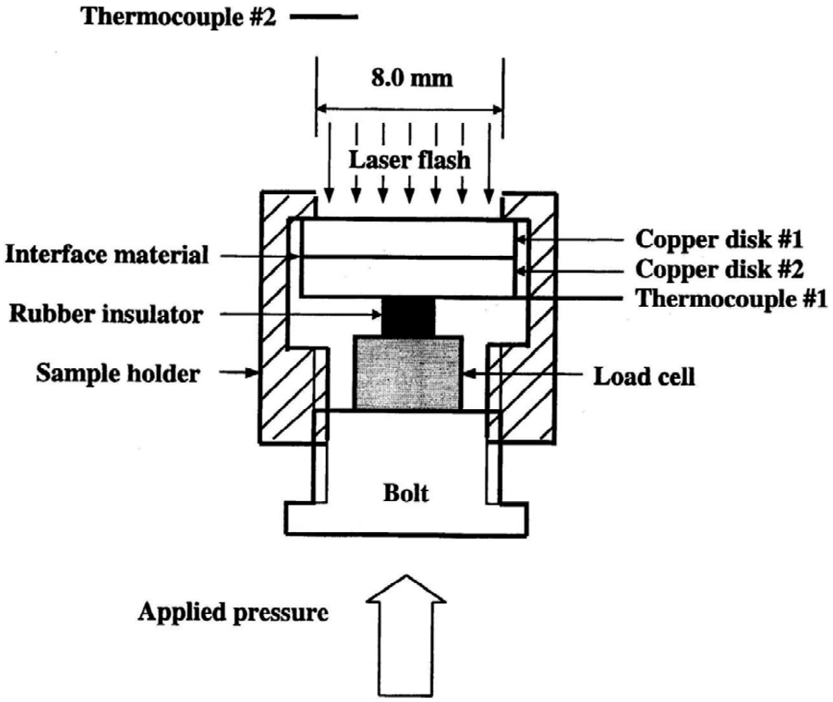

Fig. 1. Experimental set-up for thermal contact conductance measurement.

Visual Basic, was used to monitor the response of both thermocouples simultaneously. A plexiglass holder (Fig. 1) was used to facilitate pressure application. A Sensotec (Columbus, OH, USA) Model 13 load cell was used for pressure measurement. Calibration using a standard NBS 8426 graphite disk (thickness=2.62 mm) was performed before testing each specimen in order to ensure measurement accuracy. The data acquisition rate used for each test was adjusted so that there were at least 100 temperature data points during the temperature rise.

The experimental error in a transient thermal contact conductance measurement consists of random error due to experimental data scatter, and systematic error mainly due to the lag of the thermocouple response and partly due to the method used to calculate the conductance from the temperature data. The higher the thermal contact conductance, the greater is the error. The thermal diffusivity of a standard NBS 8426 graphite disk, which had a similar transient temperature rise time as the copper sandwich with the highest thermal contact conductance, was measured prior to testing each specimen in order to determine the systematic error, if any. The random error shown from the ± value was determined from measurement for five individual specimens.

This work uses thermal contact conductance (in W/m^2 °C units) to describe the quality of the thermal contact, because this quantity does not depend on the area of the contact. An alternate description is the thermal resistance (in °C/W units), which is given by:

$$\text{Thermal resistance} = \frac{1}{(\text{Thermal contact conductance}) \times (\text{Contact area})}$$

The thermal resistance is a quantity that depends on the contact area. For a thermal contact conductance of 30×10^4 W/m^2 °C (best case in this paper) and for a circular contact area of diameter 12.6 mm, the thermal resistance is 0.026 °C/W.

2.3. Viscosity testing

The viscosities of the pastes were measured at room temperature by using a rotational viscometer (Brookfield Engineering Laboratories, Middleboro, MA, USA, Model LVT dial-reading viscometer, equipped with a Model SSA-18/13R small sample adaptor).

2.4. Thermal stability testing

The thermal stability of selected pastes was tested by thermogravimetry, which consisted of heating in air from room temperature to 150 °C at a rate of 2 °C/min. A Perkin-Elmer (Norwalk, CT, USA) TGA7 instrument was used.

3. Results and discussion

3.1. Thermal contact conductance

Tables 1 and 2 give the thermal contact conductances measured for different thermal pastes.

Without carbon black, the optimum ethyl cellulose content for attaining high thermal contact conductance using PEG was 5 vol.% (Table 1). The conductance was less when the ethyl cellulose content was below or above this value. This is attributed to the increase in both conductivity and viscosity provided by the ethyl cellulose. The conductivity helped the contact conductance, thus causing the conductance to increase as the cellulose content increased from 0 to 5 vol.%. On the other hand, the viscosity was detrimental to the contact conductance, thus causing the conductance to decrease as the cellulose content increased from 5 to 15 vol.%.

The addition of carbon black to PEG containing 3 vol.% ethyl cellulose increased the contact conductance, provided that the carbon black content was 1.25 vol.% or below (Table 1). Exceeding this content caused the contact conductance to drop, as shown for a carbon black content of 1.5 vol.%, which gave an even lower conductance than in the case without carbon black. In the case of PEG containing 5 vol.% ethyl cellulose, the conductance was diminished greatly by the addition of carbon black (even just 0.5 vol.% carbon black). This is attributed to the high viscosity when ethyl cellulose was present at 5 vol.% and the further increase in viscosity upon carbon black addition. The viscosity results are described in Section 3.2. Among the PEG-based pastes, the highest contact conductance of 30×10^4 W/m^2 °C was attained by using 3 vol.% ethyl cellulose and 1.25 vol.% carbon black.

For butyl ether without carbon black the optimum ethyl cellulose content for attaining high contact conductance was 30 vol.% when the contact pressure was 0.46 MPa and was 20 vol.% when the pressure was 0.69 or 0.92 MPa. Due to its low viscosity, butyl ether dissolved ethyl cellulose more easily than PEG. However, the conductance attained by butyl ether, whether with or without ethyl cellulose, is considerably lower than that attained by PEG, whether with or without carbon black (Table 1).

The addition of carbon black to butyl ether had little effect on the contact conductance, unless the ethyl cellulose content was high (40 vol.%). In this case, the conductance increased with carbon black content from 0 to 0.20 vol.% and decreased with carbon black content from 0.20 to 0.53 vol.%. The optimum carbon black content was 0.20 vol.%, at which the conductance reached 28×10^4 W/m^2 °C.

For pastes based on PEG (with 3 vol.% ethyl cellulose) and butyl ether (with 40 vol.% ethyl cellulose), the conductance was maximum at an intermediate content of carbon black. This trend had been previously reported for boron nitride particle pastes based on lithium doped PEG

Table 1

Thermal contact conductance for various thermal pastes (containing 0–3.20 vol.% carbon black) between copper disks at various contact pressures

Thermal interface material			Conductance (10^4 W/m^2 °C)		
Vehicle	Vol.% EC	Vol.% CB	0.46 MPa	0.69 MPa	0.92 MPa
PEG	0	0	11.00±0.30	/	/
PEG	3	0	12.02±0.86	13.98±1.06	15.57±1.03
PEG	5	0	18.51±0.83	18.92±0.91	20.74±1.52
PEG	7.5	0	17.61±0.11	17.60±0.75	19.21±0.79
PEG	10	0	12.31±0.52	12.29±0.61	14.69±0.80
PEG	15	0	4.14±0.25	4.41±0.07	4.59±0.33
PEG	3	0	12.02±0.86	13.98±1.06	15.57±1.03
PEG	3	0.5	15.45±0.94	17.67±1.09	19.10±0.43
PEG	3	1.0	18.83±1.08	19.41±1.38	22.81±1.12
PEG	3	1.25	29.90±0.79	28.98±2.11	29.63±1.92
PEG	3	1.5	9.92±0.57	11.50±0.90	12.29±1.06
PEG	5	0	18.51±0.83	18.92±0.91	20.74±1.52
PEG	5	0.5	9.00±0.14	13.16±0.19	13.28±0.07
PEG	5	0.75	11.71±0.44	12.90±0.31	14.83±0.63
PEG	5	1.0	10.61±0.20	11.45±0.33	11.61±0.50
BE	0	0	2.89±0.10	/	3.86±0.08
BE	10	0	3.65±0.13	4.55±0.21	5.68±0.06
BE	20	0	3.70±0.08	5.11±0.05	6.40±0.11
BE	30	0	4.60±0.28	5.08±0.15	5.54±0.21
BE	40	0	3.67±0.13	4.37±0.12	4.61±0.06
BE	0	0	2.89±0.10	/	3.86±0.08
BE	0	1.34	2.14±0.08	/	3.75±0.06
BE	0	2.14	2.85±0.04	/	3.08±0.08
BE	0	2.67	1.64±0.10	/	2.37±0.09
BE	0	3.20	1.62±0.07	/	2.32±0.06
BE	10	0	3.65±0.13	4.55±0.21	5.68±0.06
BE	10	0.53	1.10±0.06	2.99±0.06	4.42±0.06
BE	10	1.34	4.53±0.15	5.35±0.19	5.43±0.31
BE	10	2.14	3.75±0.11	4.64±0.22	4.75±0.17
BE	10	2.67	1.75±0.05	2.75±0.06	4.05±0.18
BE	20	0	3.70±0.08	5.11±0.05	6.40±0.01
BE	20	0.53	4.02±0.13	5.17±0.09	5.47±0.28
BE	20	1.34	4.13±0.13	5.25±0.16	5.52±0.11
BE	20	2.14	5.00±0.17	5.39±0.13	5.64±0.20
BE	20	2.67	1.08±0.07	1.13±0.03	1.45±0.03
BE	30	0	4.60±0.28	5.08±0.15	5.54±0.21
BE	30	0.27	3.41±0.14	3.94±0.10	4.17±0.05
BE	30	0.53	4.23±0.16	5.60±0.22	6.62±0.32
BE	30	1.07	1.65±0.02	2.13±0.05	2.88±0.07
BE	40	0	3.67±0.13	4.37±0.12	4.61±0.06
BE	40	0.10	10.90±1.10	16.19±1.02	16.93±0.12
BE	40	0.20	27.43±2.75	28.41±2.12	28.03±1.57
BE	40	0.27	18.94±0.60	24.87±1.00	25.74±1.20
BE	40	0.30	13.62±1.32	17.05±1.26	18.54±1.53
BE	40	0.40	6.02±0.58	7.68±0.10	9.56±0.62
BE	40	0.53	4.95±0.15	5.58±0.17	5.55±0.11

The interface material thickness was below 25 μm. EC = Ethyl cellulose; CB = carbon black; BE = butyl ether. The symbol "/" means that the value was not determined.

Table 2
Thermal contact conductance for thermal pastes in the form of butyl ether containing 40 vol.% ethyl cellulose and 0.27 vol.% thermally conductive solids, as tested between copper disks at various contact pressures

Thermally conductive solid	Conductance (10^4 W/m^2 °C)		
	0.46 MPa	0.69 MPa	0.92 MPa
Carbon black	18.94±0.60	24.87±1.00	25.74±1.20
Graphite (5 μm)	3.03±0.09	3.67±0.08	4.02±0.12
Graphite (1 μm)	1.52±0.03	1.77±0.04	2.04±0.05
Nickel (3 μm)	1.85±0.05	2.14±0.02	2.84±0.04
Nickel (1 μm)	0.91±0.07	2.03±0.10	2.66±0.03
Diamond (25 μm)	1.15±0.02	1.21±0.09	1.54±0.03
Carbon filaments (0.1 μm diameter)	1.09±0.03	1.32±0.02	1.51±0.03
Single-walled carbon nanotubes*	13.5±0.2	13.8±0.3	14.1±0.4

* From Ref. [55].
The interface material thickness was below 25 μm.

[8]. As noted above, this is attributed to the required compromise between thermal conductivity and viscosity, both of which increased with increasing solid content. These viscosity results are also described in Section 3.2.

The highest conductance attained by PEG-based and butyl ether-based pastes is similar. However, the optimum carbon black content is much higher for the PEG-based paste and the optimum ethyl cellulose content is much lower for the PEG-based paste. Due to the importance of a low viscosity, the use of a high ethyl cellulose content requires that of a low carbon black content, and the use of a high carbon black content requires that of a low ethyl cellulose content.

Table 2 shows that carbon black is a much more effective conductive additive than graphite, nickel and diamond particles, as well as carbon filaments, for it provides a thermal paste that gives an exceptionally high thermal contact conductance. The superiority of carbon black occurs in spite of the relatively poor thermal conductivity of carbon black. This fact is attributed to the conformability and spreadability of the paste, as enhanced by the compressibility of each carbon black agglomerate. The compressibility of carbon black and the consequent electrical connectivity attained upon squeezing have been previously reported [53]. In particular, as an electrically conductive additive to a non-conductive MnO_2 particle cathode of an electrochemical cell, carbon black resulted in a lower resistivity than carbon filament without graphitization (same as the carbon filament used in this work), due to the squeezing of the carbon black particles between adjacent MnO_2 particles [53,54]. In contrast, the other conductive solids investigated are not compressible. Carbon black is even superior to single-walled carbon nanotubes (Table 2) [55], the pastes of which were tested using the same method and equipment as used in this work. In spite of the small size and high thermal conductivity of single-walled carbon nanotubes, carbon black is superior. Conformability and spreadability are more important than thermal conductivity or size in governing thermal paste performance.

The use of solder in place of a thermal paste as a thermal interface material gave a thermal contact conductance of (20.08±0.60)×10^4 W/m^2 °C. No pressure was applied during testing. This value is consistent with that previously reported following the same testing method and configuration [8]. Thus, the optimized carbon black pastes of this work are significantly superior to solder as thermal interface materials.

The limited effectiveness of solder occurs in spite of the high thermal conductivity of solder. This is partly due to the reaction between solder and the copper disks. This reaction results in copper–tin intermetallic compounds at the solder–copper interface [56–58]. The compound formation causes the solder to not wet the copper surface [59]. This makes it more difficult for the solder to conform to the surface topography of the copper. Once again, this suggests that conformability and spreadability are more important than thermal conductivity in governing the performance of a thermal interface material.

The thermal contact conductance values reported in this paper for pastes and solder as thermal interface materials were all obtained using the same specimen configuration, testing method and data analysis algorithm. Therefore, the values are reliable on a relative scale. However, the values deviate from the true values, due to the fact that the data analysis algorithm neglects the thickness of the thermal interface material [60].

3.2. Viscosity

Table 3 shows the viscosity of selected pastes, as measured at room temperature for various appropriate shear rates. The addition of ethyl cellulose to either PEG or butyl ether monotonically increased the viscosity, as shown in the absence of carbon black. PEG alone was higher in viscosity than butyl ether alone. However, PEG

Table 3
Viscosity (cP) at room temperature for various shear rates (s^{-1})

Vehicle	Vol.% EC	Vol.% CB	Viscosity (cP)							
			0.79 s^{-1}	2.0 s^{-1}	2.6 s^{-1}	4.0 s^{-1}	6.6 s^{-1}	7.9 s^{-1}	16 s^{-1}	40 s^{-1}
PEG	0	0	/	/	/	125	/	120	120	/
PEG	3.0	0	/	/	/	160	/	145	140	/
PEG	5.0	0	/	/	/	190	/	190	195	/
PEG	7.5	0	/	/	/	240	/	250	/	/
PEG	3.0	0.50	/	/	/	175	/	185	185	/
PEG	3.0	1.25	/	/	/	200	/	195	200	/
PEG	3.0	1.50	/	/	/	210	/	210	215	/
BE	0	0	/	/	/	/	/	/	/	<10
BE	10	0	/	/	/	/	/	/	25	20
BE	30	0	580	520	/	540	/	/	/	/
BE	40	0	/	/	4,000	/	3,900	/	/	/
BE	40	0.10	/	/	4,720	/	4,400	/	/	/
BE	40	0.20	/	/	5,200	/	4,800	/	/	/
BE	40	0.30	/	/	5,600	/	5,200	/	/	/
BE	40	0.20[a]	/	/	4,000	/	3,900	/	/	/
BE	40	0.20[b]	/	/	4,800	/	4,480	/	/	/
BE	40	0.20[c]	/	/	5,000	/	4,720	/	/	/

BE = Butyl ether; EC = ethyl cellulose; CB = carbon black.

[a] Graphite particles (1 μm).

[b] Graphite particles (5 μm).

[c] Carbon filaments.

with the optimum ethyl cellulose content of 3 vol.% was much lower in viscosity than butyl ether with the optimum ethyl cellulose content of 40 vol.%. The addition of carbon black monotonically increased the viscosity, as shown for PEG containing 3 vol.% ethyl cellulose and for butyl ether containing 40 vol.% ethyl cellulose.

The PEG with 5.0 vol.% ethyl cellulose and the PEG-based paste containing 3.0 vol.% ethyl cellulose and 1.25 vol.% carbon black were similar in viscosity. The latter gave a higher contact conductance than the former, due to a decrease in the ethyl cellulose content and an increase in the carbon black content. Thus, adjustment of the contents of both ethyl cellulose and carbon black is needed in order to attain an optimized thermal paste formulation.

As shown in Table 1, the butyl ether-based paste with 40 vol.% ethyl cellulose and 0.20 vol.% carbon black and the PEG-based paste with 3 vol.% ethyl cellulose and 1.25 vol.% carbon black are the two thermal pastes that gave the highest thermal contact conductance in this study. Although the two pastes gave comparably high values of contact conductance, the butyl ether-based paste exhibited a much higher viscosity than the PEG-based paste, as shown in Table 3.

Table 3 also shows that the viscosity of the butyl ether-based paste with 40 vol.% ethyl cellulose was lower when the paste contained 0.20 vol.% graphite particles (1 or 5 μm) or carbon filaments than when it contained 0.20 vol.% carbon black. However, it was noticed during paste mixing that the carbon black paste was much smoother than the graphite particle paste. The smoothness of the paste probably relates to the wettability of carbon black. It is apparently more important than the viscosity in governing thermal paste performance. Perhaps smoothness relates more closely to the conformability than a low viscosity.

The viscosity of butyl ether-based paste with 40 vol.% ethyl cellulose and 0.20 vol.% solid increased in the order: 1 μm graphite particles, 5 μm graphite particles and carbon filaments (Table 3). This trend is consistent with the notion that a larger particle size tends to result in a paste with a higher viscosity and that filaments tend to result in a higher viscosity than particles, provided that no significant agglomeration of individual particles takes place.

Although the viscosity is useful as a suggestive indicator of thermal paste performance, it is not as relevant as the conformability, which is the attribute that really governs thermal paste performance. Since there is no standardized method to evaluate paste conformability, this work resorted to viscosity measurements.

3.3. Thermal stability

Figs. 2 and 3, respectively, show the thermogravimetric results for PEG and butyl ether (with and without ethyl

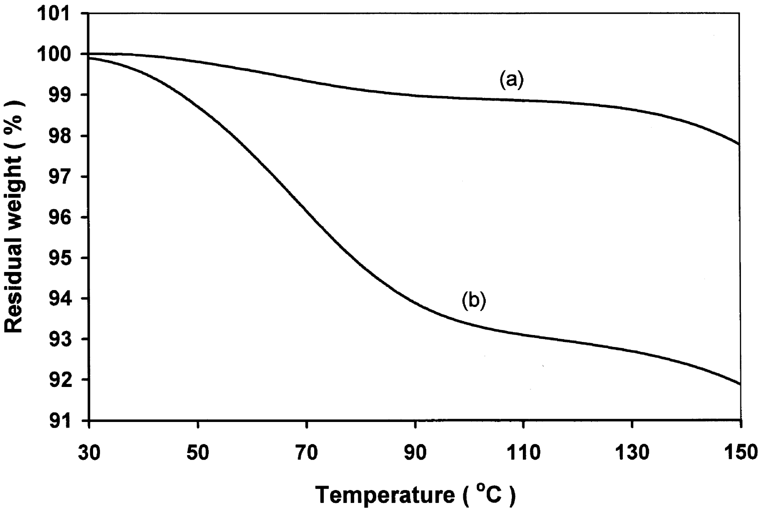

Fig. 2. Thermogravimetric results. (a) PEG by itself (initial weight = 62.11 mg). (b) PEG with 3 vol.% ethyl cellulose (initial weight = 73.98 mg).

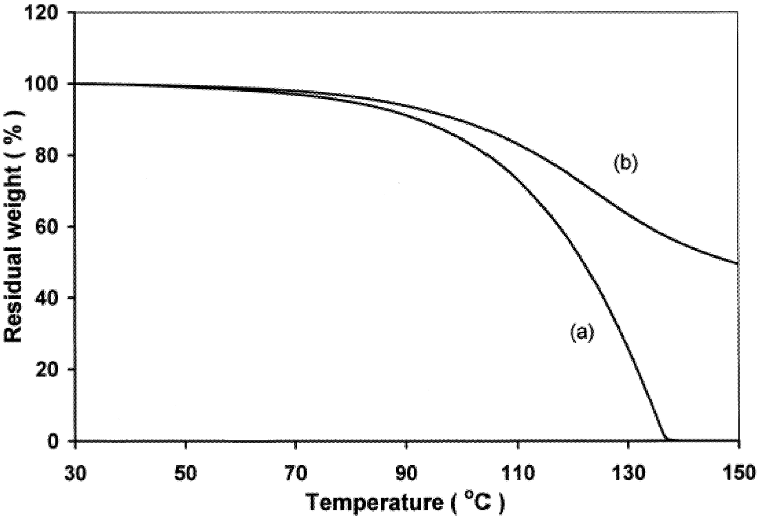

Fig. 3. Thermogravimetric results. (a) Butyl ether by itself (initial weight = 34.72 mg). (b) Butyl ether with 40 vol.% ethyl cellulose (initial weight = 42.54 mg).

cellulose in each case, but without carbon black, which does not affect the thermal stability of the dispersion, as shown by thermogravimetric analysis in this work). Without ethyl cellulose, PEG is much more stable thermally than butyl ether. The dissolution of ethyl cellulose diminished the thermal stability of PEG, but increased that of butyl ether. Table 4 shows the comparison of residual weights at three temperatures. At 50 and 75 °C, butyl ether containing ethyl cellulose is more stable thermally than PEG containing ethyl cellulose, but at 100 °C, the reverse is true. Above about 100 °C, the weight loss of butyl ether, whether with or without ethyl cellulose, is extensive (more

Table 4
Thermogravimetric results of thermal pastes

Vehicle	Vol.% EC	Residual weight (%)		
		50 °C	75 °C	100 °C
PEG	0	99.81	99.22	98.91
PEG	3	98.73	95.47	93.36
BE	0	98.98	96.11	84.67
BE	40	99.33	97.26	89.68

EC = Ethyl cellulose; BE = butyl ether.

than 50% weight loss at 150 °C). However, the weight loss remains less than 9% even at 150 °C for PEG, whether with or without ethyl cellulose. Therefore, butyl ether-based pastes are not suitable for use above 100 °C, whereas PEG-based pastes are suitable for use up to at least 150 °C.

4. Conclusions

The use of a PEG-based paste (containing 3 vol.% dissolved ethyl cellulose and dispersed carbon black in the optimum amount of 1.25 vol.%) as a thermal paste between copper disks results in a thermal contact conductance of 30×10^4 W/m^2 °C, compared to a value of 20×10^4 W/m^2 °C for tin–lead–antimony eutectic solder applied in the molten state. Almost as effective as the PEG-based paste is a butyl ether-based paste (containing 40 vol.% dissolved ethyl cellulose and dispersed carbon black in the optimum amount of 0.20 vol.%), which gives a thermal contact conductance of 28×10^4 W/m^2 °C. The PEG-based paste is superior to the butyl ether-based paste in the thermal stability at 100 °C and above, though the reverse is true at 75 °C and below. The superiority of these pastes to solder as thermal interface materials is presumably due to the reaction between solder and copper and the consequent poor conformability of molten solder with copper.

The use of PEG by itself gives a thermal contact conductance of 11×10^4 W/m^2 °C. The dissolution of ethyl cellulose at the optimum concentration of 5 vol.% increases the conductance to 19×10^4 W/m^2 °C. The use of butyl ether by itself gives a conductance of 3×10^4 W/m^2 °C only. The dissolution of ethyl cellulose at the optimum concentration of 20–30 vol.% gives a conductance ranging from 4×10^4 to 6×10^4 W/m^2 °C.

The addition of carbon black to PEG helps the conductance only when the ethyl cellulose is at 3 vol.% and the carbon black content is at 1.25 vol.% or below. The addition of carbon black to PEG degrades the conductance when the ethyl cellulose is at 3 vol.% and the carbon black is at 1.5 vol.%, or when the ethyl cellulose is at 5 vol.%. These effects are presumably due to the importance of conformability and spreadability toward the performance of thermal pastes. Both carbon black and ethyl cellulose cause the viscosity of the pastes to increase, so excessive amounts of these ingredients degrade the conductance. The optimum carbon black content is higher for PEG than butyl ether, whereas the optimum ethyl cellulose content is higher for butyl ether than PEG. In spite of the difference in carbon black content, the thermal contact conductance at room temperature is similar between the optimized PEG-based paste and the optimized butyl ether-based paste. Since carbon black is the ingredient in the paste that is most conductive thermally, this implies that the conformability and spreadability are more important than the thermal conductivity in governing the thermal paste performance.

In spite of its relatively low thermal conductivity, carbon black is much more effective than graphite, nickel and diamond particles and carbon filaments, all evaluated at the same volume fraction, for providing thermal pastes. This is attributed to the compressibility of a carbon black agglomerate and the consequent conformability and spreadability of the paste.

Acknowledgements

The authors thank Professor Yunsheng Xu of Winona State University for technical assistance.

References

[1] Wolff EG, Schneider DA. Prediction of thermal contact resistance between polished surfaces. Int J Heat Mass Transfer 1998;41(22):3469–82.

[2] Ouellette T, de Sorgo M. Thermal performance of heat transfer interface materials. In: Proceedings of the Power Electronics Design Conference, Power Sources Users Conference, Cerritos, CA; 1985, pp. 134–8.

[3] Vogel MR. Thermal performance for a miniature heat sink cooled by microPCM slurry. In: Proceedings of the International Intersociety Electronic Packaging Conference, Advances in Electronic Packaging, New York: American Society of Mechanical Engineers; 1995, p. 989, vol. 10-2.

[4] Wilson SW, Norris AW, Scott EB, Costello MR. Thermally conductive adhesives for highly thermally stressed assembly. In: National Electronic Packaging and Production Conference, Proceedings of the Technical Program, Norwalk, CT: Reed Exhibition Companies; 1996, pp. 788–96, vol. 2.

[5] Peterson AL. Silicones with improved thermal conductivity for thermal management in electronic packaging. In: Proceedings of the 40th Electronic Components and Technology Conference, Piscataway, NJ: IEEE; 1990, pp. 613–9, vol. 1.

[6] Lu X, Xu G, Hofstra PG, Bajcar RC. Moisture-absorption, dielectric relaxation, and thermal conductivity studies of polymer composites. J Polym Sci, Part B 1998;36(13):2259–65.

[7] Sasaski T, Hisano K, Sakamoto T, Monma S, Fijmori Y, Iwasaki H et al. Development of sheet type thermal conductive compound using AlN. In: Japan IEMT Symposium Proceedings, IEEE/CPMT International Electronic Manufacturing Technology (IEMT) Symposium, Piscataway, NJ: IEEE; 1995, pp. 236–9.

[8] Xu Y, Luo X, Chung DDL. Lithium doped polyethylene-glycol-based thermal interface pastes for high thermal contact conductance. J Electron Packaging 2002;124(3):188–91.

[9] Xu Y, Luo X, Chung DDL. Sodium silicate based thermal pastes for high thermal contact conductance. J Electron Packaging 2000;122(2):128–31.

[10] Galli E. Carbon blacks. Plastics Compounding 1982;5(2):22–32.

[11] Helsen JA, Teixeira J. Fractal behaviour of carbon black and smectite dispersions by small angle neutron scattering. Colloid Polym Sci 1986;264(7):619–22.

[12] Mewis J, de Groot LM, Helsen JA. Dielectric behaviour of flowing thixotropic suspensions. Colloids Surf 1987;22(2–4):271–89.

[13] Genz U, Helsen JA, Mewis J. Dielectric spectroscopy of reversibly flocculated dispersions during flow. J Colloid Interface Sci 1994;165(1):212–20.

[14] Ishii C, Koseki K, Amari T, Hanzawa Y, Yoshizawa N, Hatori H et al. Flow behavior of graphitized carbon black suspensions. Carbon 2001;39(15):2384–6.

[15] Trappe V, Weitz DA. Scaling of the viscoelasticity of weakly attractive particles. Phys Rev Lett 2000;85(2):449–52.

[16] Kratohvil S, Matjevic E. Stability of carbon suspensions. Colloids Surf 1982;5(3):179–86.

[17] Fitzgerald ER, Ferry JD. Dynamic mechanical properties for carbon black-in-oil-analysis of frequency and temperature dependence. Rubber Chem Technol 1982;55(5):1569–77.

[18] Amari T. Non-linear viscoelastic properties of concentrated suspensions. Prog Org Coatings 1997;31(1–2):11–9.

[19] Kumar U. A development methodology for copper end termination paste—part 1: origin of green defects. Active Passive Electron Components 2002;25(2):169–79.

[20] Chae K-S, Choi H-K, Ahn J-H, Song Y-S, Lee DY. Effect of organic vehicle addition on service lifetime of Ti/IrO_2–RuO_2 electrodes. Mater Lett 2002;55(4):211–6.

[21] Heller A, Schaffrath W, Otschik P. Effect of surfactants on the flow behavior of pastes. Tenside, Surfact Detergents 1992;29(5):315–9.

[22] Stanton RM. Rheological aspects of thick film technology; an investigation of the flow properties of ethyl cellulose vehicle system. Int J Hybrid Microelectron 1983;6(1):419–32.

[23] Bernazzani L, Ceccanti N, Conti G, Gianni P, Mollica V, Tine MR. Volumetric properties of (an organic compound + di-*n*-butyl ether) at $T = 298.15$ K. J Chem Thermodynamics 2001;33(6):629–41.

[24] Khare PK, Jain SK, Paliwal SK. Ageing effect on ethyl cellulose films. Polym Int 1997;42(2):138–42.

[25] Khare PK, Pandey RK, Chourasia RR, Jain PL. Transient and steady-state conduction in ethyl cellulose (EC)–poly-(methyl methacrylate) (PMMA) blends. Polym Int 2000;49(7):719–27.

[26] Nakamura S, Ito A, Sawa G, Orita S, Tubota K. Approach of obtaining low temperature coefficient of resistance in carbon black-epoxy resin resistors. NEC Res. Dev. 1986;(83):121–7.

[27] Saad ALG, Sayed WM, Ahmed MGM, Hassan AM. Preparation and properties of some filled poly(vinyl chloride) compositions. J Appl Polym Sci 1999;73(13):2657–70.

[28] Takino H, Takahashi H, Yamano K, Kohjiya S. Effects of carbon black and process oil on viscoelastic properties and tire wet skid resistance. Tire Sci Technol 1998;26(4):241–57.

[29] Haws JR, Wilder CR, Middlebrook TC. Effect of carbon black properties on the rolling resistance of tires. In: Rubber Division Symposia, Akron, OH: ACS; 1982, pp. 257–81, vol. 1.

[30] Hess WM, Klamp WR. Effects of carbon black and other compounding variables on tire rolling resistance and traction. Rubber Chem Technol 1983;56(2):390–417.

[31] Kundu PP, Kukreja TR. Surface modification of carbon black by vegetable oil—its effect on the rheometric, hardness, abrasion, rebound resilience, tensile, tear, and adhesion properties. J Appl Polym Sci 2002;84(2):256–60.

[32] Ramesan MT, Premalatha CK, Alex R. Influence of carbon black on uncompatibilised and compatibilised SBR–NBR blends. Plastics Rubber Composites 2001;30(8):355–62.

[33] Sridhar V, Prasad K, Choe S, Kundu PP. Optimization of physical and mechanical properties of rubber compounds by a response surface methodological approach. J Appl Polym Sci 2001;82(4):997–1005.

[34] Takei K, Terada N, Kumai K, Iwahori T, Uwai T, Miura T. Effects of the macroscopic structure of carbon black on its behaviour as the anode in a lithium secondary cell. J Power Sources 1995;55(2):191–5.

[35] Van Deraerschot R, Van Den Bergh F, Smet H. Special type of carbon black as substitute for acetylene black in dry cells. In: Electrochemical society extended abstracts, vol. 84–2, Pennington, NJ: Electrochemical Society; 1984, p. 139.

[36] Erhan SZ, Bagby MO. Lithographic and letter press ink vehicles from vegetable oils. J Am Oil Chem Soc 1991;68(9):635–8.

[37] Bratkowska I, Zwierzykowski W. Influence of raw materials on rheological properties of carbon black dispersion in mineral oil utilised for printing inks production. Przemysl Chemiczny 1987;66(8):393–5.

[38] Bratkowska I, Zwierzykowski W. Carbon-black suspension for print ink production. Przemysl Chemiczny 1986;65(7):363–5.

[39] Chinas-Castillo F, Spikes HA. Behavior of colloidal solid particles in elastohydrodynamic contacts. Tribol Trans 2000;43(3):387–94.

[40] Shiao SJ, Fu WS, Tuo CL, Cheng UI. Polymer-based self-lubricating material. J Appl Polym Sci 2001;80(9):1514–9.

[41] Kozlovtsev AP, Serova TM, Batyshtova KM, Khramkov VP, Zayats NN. Lubrication oils for glass-shaping machine molds (review). Glass & ceramics (English translation of Steklo I Keramika) 1988;45(3–4):154–7.

[42] Bakaleinikov MB, Nikonorov EM. Rheological properties of high-temperature lubricating greases. Chem Technol Fuels Oils 1982;18(3–4):108–11.

[43] Srivastava RK, Linak WP. Evaluation of carbon black slurries as clean burning fuels. Fuel 1994;73(12):1911–7.

[44] Steinberg M. Low cost high energy density carbon black fuel mix for heat engines. In: Preprints, vol. 32, Washington, DC: Division of Petroleum Chemistry, American Chemical Society; 1987, pp. 565–71, Nos. 1–2.

[45] Smith CA. Running-in additives and slurries: effects on improved fuel economy. Automotive Eng (London) 1982;7(1):23–4;
Smith CA. Running-in additives and slurries: effects on improved fuel economy. Automotive Eng (London) 1982;7(1):27.

[46] Ueki MM, Zanin M. Influence of titanium dioxide and carbon black on the high density polyethylene DC breakdown strength evaluated by Weibull distribution. In: Proceedings of the 1997 Annual Conference on Electrical Insulation and Dielectric Phenomena, Annual report, vol. 1, Piscataway, NJ: IEEE; 1997, pp. 173–6.

[47] Ueki MM, Zanin M. Relationship between different mixing conditions and DC breakdown strength of high density polyethylene compound. In: Proceedings of the 1997 Annual

Conference on Electrical Insulation and Dielectric Phenomena, Annual report, vol. 1, Piscataway, NJ: IEEE; 1997, pp. 170–2.

[48] Lockett GE. Heat pipes to tap geothermal energy. H & V Eng 1986;59(676):7–8.

[49] Lockett GE. Hot rock geothermal energy extraction unit for single borehole technology. In: Proceedings of the European Congress, Energy economics and management in industry, vol. 1, Oxford, New York: Pergamon Press; 1984, pp. 285–9.

[50] Dawes AG, Milner CN, Peirce TJ. Development of a prototype fluidised bed thermal fluid heater. In: Fluidised combustion: is it achieving its promise?, vol. 1, London: Institute of Energy; 1984, Pap KN/III/2.

[51] Parker WJ, Jenkins RJ, Butler CP, Abbott GL. Flash method of determining thermal diffusivity, heat capacity and thermal conductivity. J Appl Phys 1961;32(9):1679–83.

[52] Inoue K, Ohmura E. Measurement by laser flash method of thermal diffusivity of two-layer composites. Yosetsu Gakkai Ronbunshu/Q J Jpn Welding Soc 1988;6(3):130–4.

[53] Frysz C, Shui X, Chung DDL. Carbon filaments and carbon black as a conductive additive to the manganese dioxide cathode of a lithium electrolytic cell. J Power Sources 1996;58(1):41–54.

[54] Lu W, Chung DDL. A comparative study of carbons for use as an electrically conducting additive in manganese dioxide cathode of an electrochemical cell. Carbon 2002;40(ER3):447–9.

[55] Xu Y, Leong CK, Chung DDL. Nanotechnology, in press.

[56] Grivas D, Frear D, Quan L, Morris Jr. JW. The formation of Cu_3Sn Intermetallic on the reaction of Cu with 95Pb–5Sn solder. J Electron Mater 1986;15(6):355–9.

[57] Tu KN. Cu/Sn interfacial reactions: thin-film case versus bulk case. Mater Chem Phys 1996;46:217–23.

[58] Tsutsumi K, Kohara M, Shibata H, Nakata H. Study of the tin–copper metallurgical reaction at solder bumps. Int J Hybrid Microelectron 1984;7(4):38–43.

[59] Kim HK, Wang Y, Maheshwari A, Tu KN. Wetting behaviors of Sn-based solders on Cu and Pd surfaces. In: Sundahl RC, Tu K-N, Jackson KA, Borgensen P, editors, Materials research society symposium proceedings, Vol. 390, Materials Research Society; 1995, pp. 183–8.

[60] Luo X, Chung DDL. Effect of the thickness of a thermal interface material (solder) on heat transfer between copper surfaces. Int J Microcircuits Electron Packaging 2001;24(2):141–7.